

# The Coherence Time of Midtropospheric Wind Features as a Function of Vertical Scale from 300 m to 2 km

FRANCIS J. MERCERET

*National Aeronautics and Space Administration Kennedy Space Center, Florida*

(Manuscript received 28 August 1999, in final form 4 March 2000)

## ABSTRACT

The coherence between vertical wind profiles separated by a time lag is measured as a function of vertical scale from Doppler radar wind profiler data. Each profile covers altitudes from 6811 m to 16 261 m and is Fourier transformed over a vertical wavenumber (inverse scale) range from 0 to  $3.33 \times 10^{-3} \text{ m}^{-1}$ . Time lags between profiles of 0.083, 0.25, 0.5, 1.0, and 2.0 h are used. A correction for instrument noise is derived and is applied to the results. An empirical formula for the coherence as a function of lag and scale is presented and evaluated. The “coherence time” is defined as the value of time lag beyond which the coherence decays below a chosen value at a given scale. A relation between coherence time and vertical scale is derived. This relation provides a measure of the lifetime of wind features in the midtroposphere as a function of their vertical scale for application to space vehicle wind loads.

## 1. Introduction

There is an ongoing discussion within the space launch community about the measurement of upper-air winds. The discussion centers on what vertical resolution is actually required for operational decision making. If the lifetime of the fine structure is less than the time between when measurements are taken and launch (typically 0.5–2 h), then the measured fine structure is not operationally significant since it will not be the fine structure encountered by the vehicle on ascent. This paper is an attempt to quantify the lifetime of features in the midtroposphere (where vehicle wind loads are most important) as a function of their vertical scale. The results may be used as a guide to determining the resolution required of upper-air wind instruments supporting spaceflight operations.

The paper begins with a description in section 2 of the data and methodology used to perform the analysis, including the instrument and software used to acquire the data. Section 3 and the appendix provide a method for correcting atmospheric coherence measurements for instrument noise provided both the signal and the noise have certain specified spectral characteristics. Section 4 presents an empirical model for the coherence of the  $u$  and  $v$  components of the wind as a function of vertical wavenumber and time lag. The model is applied to both

the corrected and the uncorrected correlation measurements. Using the model, the desired relation between lifetime and vertical scale is derived. The paper concludes with a brief summary and some concluding remarks in section 5.

## 2. Data and methodology

The launch community’s concept of “lifetime” for atmospheric features needed to be defined specifically before its relationship to vertical scale could be examined quantitatively. For this study, the coherence time,  $\tau$ , is the measure of lifetime. It is that time lag beyond which the coherence drops below a chosen value,  $\epsilon$ , at the vertical scale in question. The term “coherence” is sometimes used to mean the cross spectrum divided by the square root of the product of the power spectra, and sometimes to mean the square of that quantity. The latter is preferred by the author and is used here. Thus the quantity called coherence in this paper is called “coherence squared” by Wilfong et al. (1997).

The data were collected using the Kennedy Space Center (KSC) 50-MHz Doppler radar wind profiler (DRWP). The profiler and its associated software are described in detail in Schumann et al. (1999) but for convenience a summary is included here. The DRWP uses a vertical beam and two oblique beams inclined  $15^\circ$  from the vertical at azimuths of  $45^\circ$  and  $135^\circ$ . The beams are scanned sequentially with a dwell time of 103 s in each beam. The operating frequency is 49.25 MHz, corresponding to a free space wavelength of 6.085 m. The beam width is  $2.9^\circ$ . The altitude range from

---

*Corresponding author address:* Francis J. Merceret, NASA, YA-D, Kennedy Space Center, FL 32899.  
E-mail: francis.merceret-1@ksc.nasa.gov

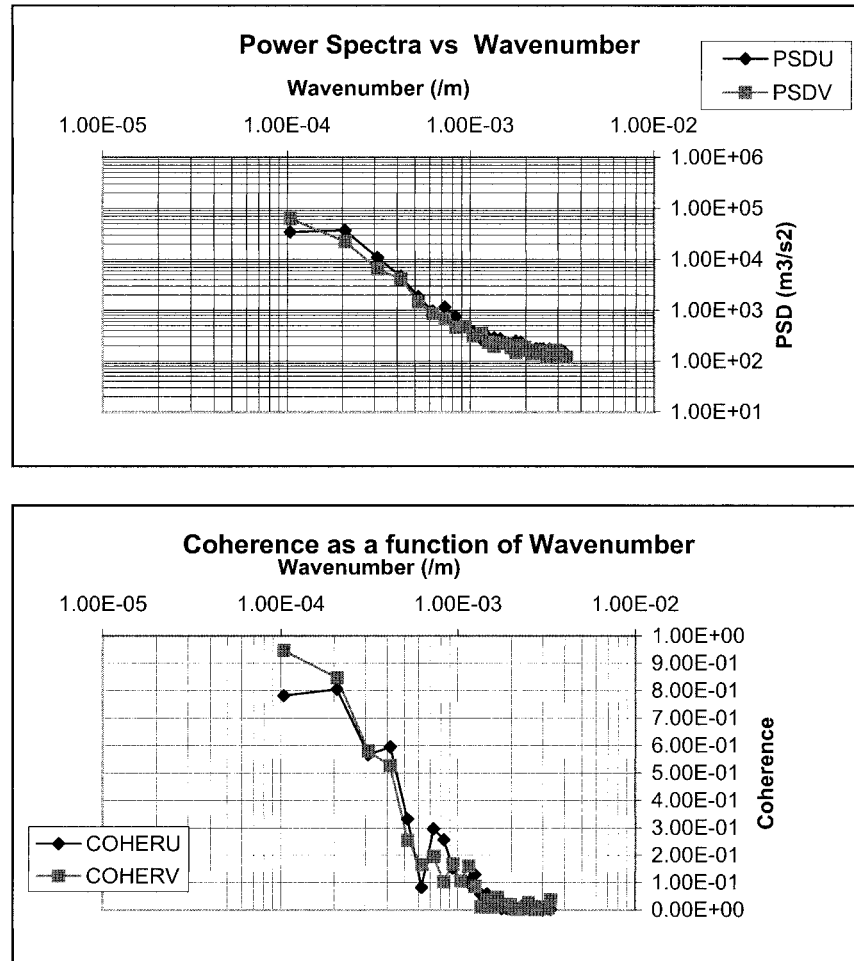


FIG. 1. Power and coherence spectra from a "normal" day (3 Jan 1996) for a time lag of 0.5 h (six profiles). The sample size is 271 profiles. In this and the following figures, PSD means power spectral density.

2011 to 18 661 m is covered in 112 range gates of 150-m thickness. The pulse length is  $8 \mu\text{s}$  with 8-bit pulse coding and a pulse repetition period of  $160 \mu\text{s}$ . Coherent averaging of 256 pulses is performed prior to a 256-point Fourier transform to generate each raw Doppler spectrum. Eight raw Doppler spectra are averaged to produce the spectrum to be processed for winds.

Winds are generated from the radar spectra using the median filter first guess (MFFG) algorithm developed by Wilfong et al. (1993) and implemented at KSC by the Applied Meteorology Unit. Its structure and performance are described in minute detail by Schumann et al. (1999) from which the following material is taken. Unlike the hardware, this software package is not easy to summarize briefly. The key elements are application of a temporal median filter to the Doppler spectrum at each range gate, and the use of a "first-guess" window to constrain the search for the wind signal in the filtered Doppler spectrum. The algorithm has demonstrated very high reliability and an rms accuracy on the order of 1

$\text{m s}^{-1}$  in intercomparisons with high resolution wind sounding balloons (jimspheres). The wind computations do not use the vertical wind information because the vertical winds in central Florida are so small that the use of the vertical beam adds more noise than signal to the result.

The same data used by Merceret (1999) are used in this study. The data are a subset of those prepared by Merceret (1997) for a study of wind change probabilities. They had been screened through an extensive automated and manual quality control (QC) process. This QC included automated reasonableness tests, gradient tests, signal-to-noise-ratio tests, and time-height continuity checks. After the automated QC, a visual inspection of a color-contour presentation of every daily record was performed. Data that failed to meet any of the acceptance criteria were not included in the analysis. See Merceret (1997) for details. Less than 0.5% of the data in the complete set were eliminated by this process.

Analysis of the vertical beam-derived velocities for

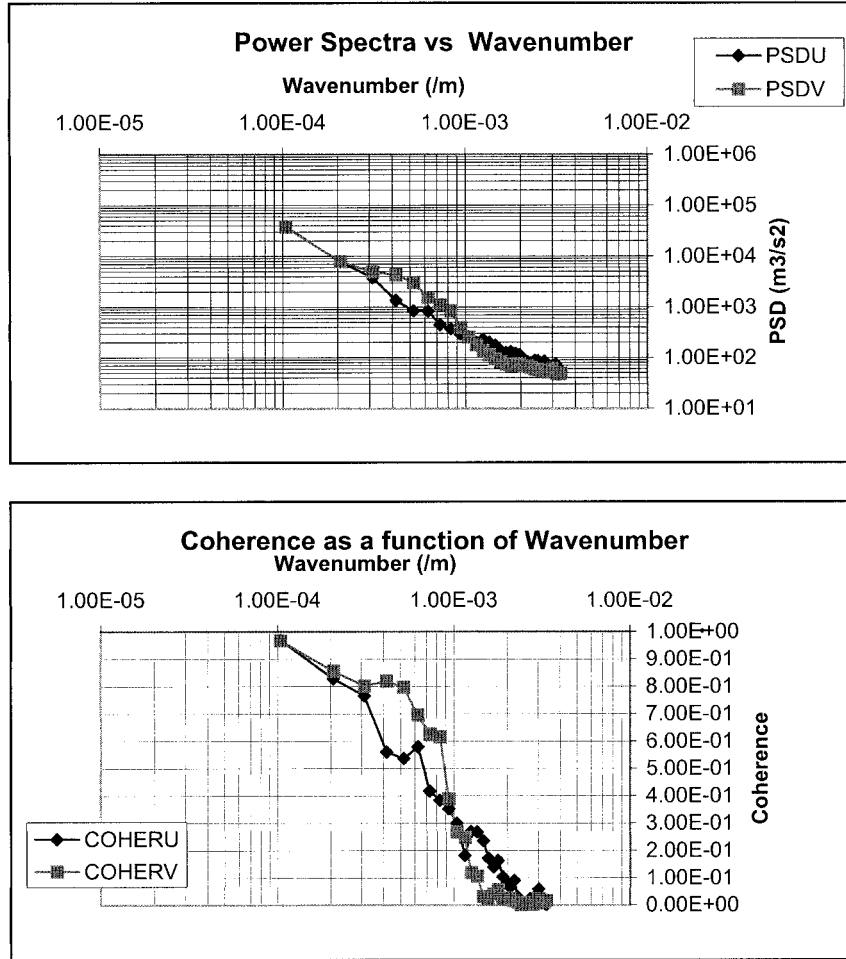


FIG. 2. Power and coherence spectra from an anomalous day (10 Dec 1995) for a lag of 0.5 h. The sample size is 262 profiles.

these data showed a mean of  $0.0016 \text{ m s}^{-1}$  with a standard deviation of  $0.37 \text{ m s}^{-1}$ , which is less than the average spectral width of  $0.65 \text{ m s}^{-1}$ . The frequency of the magnitude of the measured vertical velocity exceeding  $1 \text{ m s}^{-1}$  was 0.006, the frequency of exceeding  $2 \text{ m s}^{-1}$  was less than 0.0005 and none exceeded  $3.4 \text{ m s}^{-1}$ . Thus the neglect of the vertical velocities in the data processing appears justified.

Ninety-three days, each having at least 100 consecutive profiles, constitute the sample. Each profile contains wind speed and direction at 112 adjacent "gates" 150 m apart beginning at an altitude of 2011 m. The  $u$  and  $v$  components were computed for gates 33–96 in each profile and a fast Fourier transform (FFT) was applied separately to the  $u$  and  $v$  components. This covers the altitude range from 6811 to 16 261 m in 64 steps and yields spectra covering wavenumbers from 0 to  $0.00333 \text{ m}^{-1}$  in 32 steps. The number of steps was selected as a power of 2 to accommodate existing FFT software. The altitude range was selected to cover the

range of maximum concern for large launch vehicles on ascent.

Profiles were processed in pairs spaced  $L$  hours apart where  $L = 0.083, 0.25, 0.5, 1$  and  $2$ . From the FFTs, the power spectrum and cross spectrum between the current profile and the time-lagged profile were computed for both components. Before taking transforms, the mean and linear trend were removed from each set of data and a triangular window (Parzen 1961) was applied. For each day in the sample, the average power spectra of  $u$  and  $v$  plus the coherence spectra of  $u$  and  $v$  with respect to the time-lagged profiles was computed. Data from multiple days were combined by sample-size-weighted averaging of the power and coherence spectra.

All of the data were taken in the winter season (October–March) and constitute a representative sample of that season. The results obtained here may not apply to the summer season, which is characterized by lighter winds aloft and smaller wind shear values.

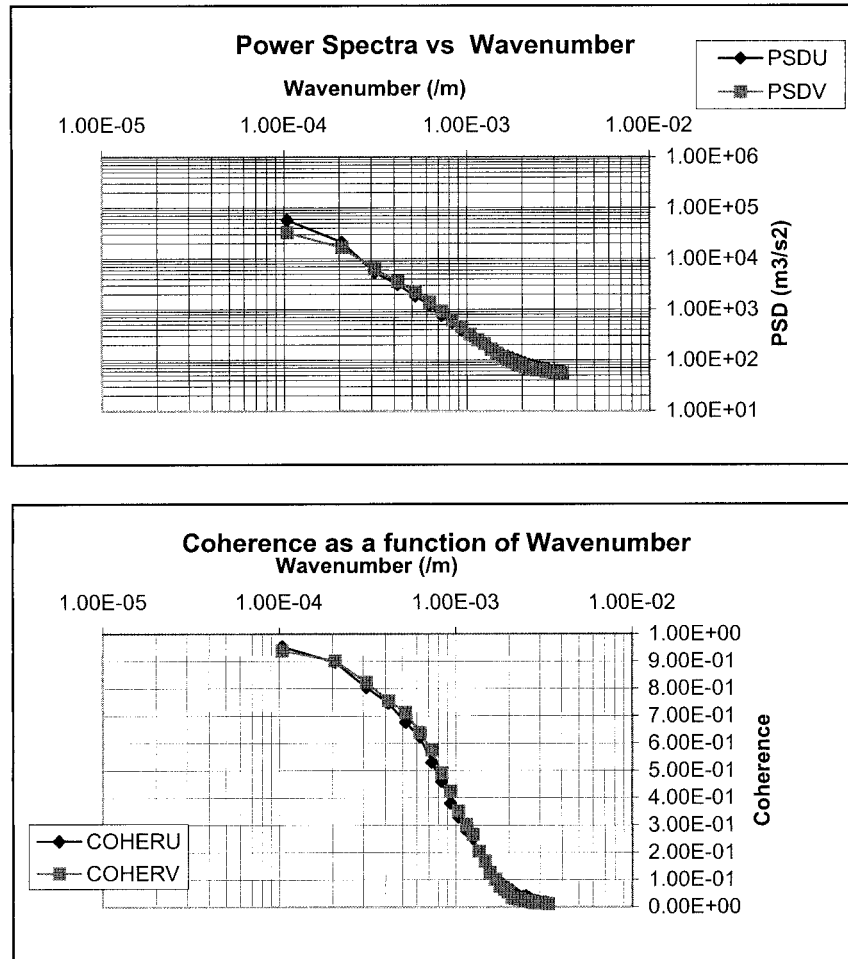


FIG. 3. Power and coherence spectra for the average of all days in the set for lag = 0.5 h. There were 93 days and 22 260 profiles in the average.

### 3. Correcting the coherence spectra for instrument noise

A proper analysis of coherence time versus vertical scale requires that the actual coherence be known, but all that is available is the measured coherence. The measured coherence will be lower than the actual coherence if the output from the measuring instrument contains any incoherent noise. If the atmospheric signal and the noise satisfy certain assumptions, then the measured coherence may be corrected for the effects of the noise. A detailed derivation is given in the appendix. Noise means anything which is not part of the signal, regardless of its source.

If we assume that the noise spectrum is independent of frequency (“white noise”) and that the signal spectrum obeys a power law  $\langle SS^* \rangle \propto (k/k_0)^{-\beta}$  (“red noise” typical of atmospheric signals), then we can write the correction as

$$C_{\text{actual}}(k) = C_{\text{measured}}(k)[1 + (\sqrt{2} - 1)(k/k_0)^\beta]^2, \quad (1)$$

where  $k_0$  is the frequency at which the measured coherence falls to 0.5 for a perfectly coherent signal.

In the inertial subrange, wind spectra obey a power law with  $\beta = 5/3$  (Stull 1989; Lumley and Panofsky 1964). At larger scales in the buoyancy subrange, there is no universal power law (Weinstock 1978). Midtropospheric power law vertical spectra with slopes from  $\beta = 1.6$  to  $\beta = 3$  over scales of relevance here have been reported (Wilfong et al. 1997; Nastrom et al. 1997). The observed variation is thought to result from the presence of a gravity wave continuum that leads to  $\beta = 3$  when fully saturated (Nastrom et al. 1997; Allen and Vincent 1995). Some of the variance may also be due to spectral distortion in balloon measurements due to their slow rise rate (Alexander and De La Torre 1999). The observed power spectra for the datasets used here also appear to obey power laws with slopes ranging between 1.6 and 3 with an average above 2. This range of exponents makes little difference in the results derived below.

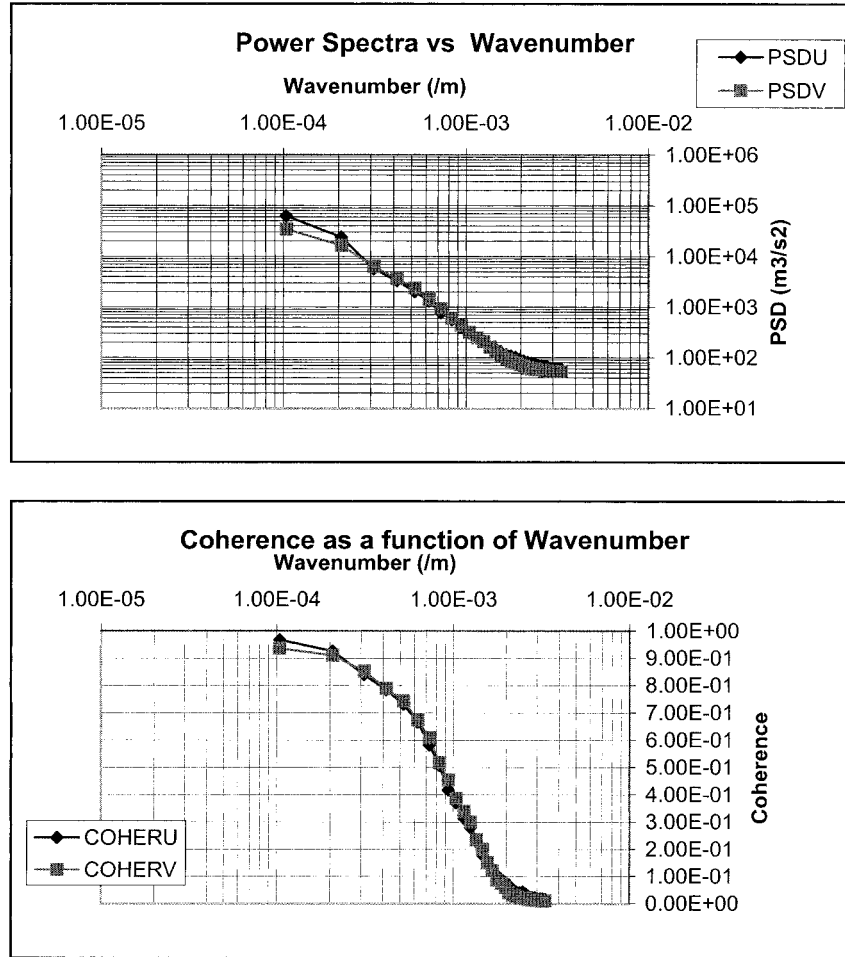


FIG. 4. Power and coherence spectra of the average of all normal days for lag = 0.5 h. There were 62 days and 15 172 profiles in the average.

**4. The coherence model**

When originally conceived, this study was expected to involve quick calculations of the coherence scale directly from the measurements for each of the target lag times. The final product was to be a two-dimensional plot of lag time versus scale. While exploring techniques for correcting the coherence measurements for the effects of instrument noise, an empirical function that appeared to fit the data was found. The resulting three-dimensional model provides a much more complete picture of the “lifetime” of features as a function of scale and lag.

*a. The raw data*

The power spectra and coherence functions for some days exhibited peaks suggesting the presence of wave-like phenomena and other days showed evidence of “spectral leakage” due to the signal processing used as described in Merceret (1999). This suggested selection

of a subset of the data representative of the turbulent atmosphere in the absence of waves since it was not obvious that the same model would work in both cases. The author selected these days subjectively based on the shapes of the power and coherence spectra. Days with significant anisotropy between the *u* and *v* components, or having peaked or odd-shaped spectra were designated anomalous. An example of a “normal” day for a lag of 0.5 h is presented in Fig. 1 and an anomalous day is shown in Fig. 2. Note that the *u* and *v* power spectra and coherences in Fig. 2 differ. The *v* spectrum and coherence both contain a peak not present on a normal day. The shape of the *v* spectrum does not follow a power law either. The average of all of the data for a lag of 0.5 h is shown in Fig. 3 while the average of the normal days is shown in Fig. 4.

The coherence as a function of wavenumber and lag for the *u* component for an average of all of the data is shown in Fig. 5. The empirical function that fits this surface is shown in Fig. 6. The formula is

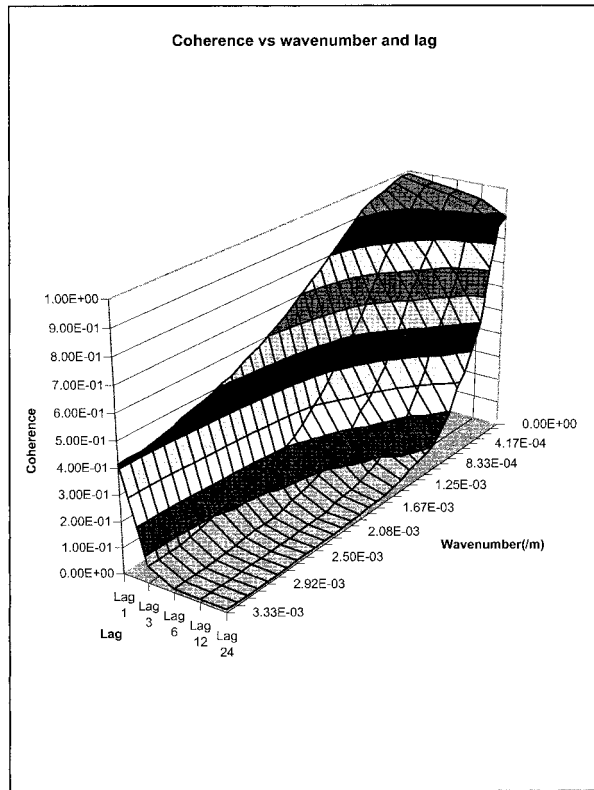


FIG. 5. Coherence as a function of vertical wavenumber and time lag for the  $u$  component. All data were used. Lag  $N$  denotes a lag of  $N$  profiles. The lag value in hours =  $N/12$ . There are 93 days with over 20 000 profiles represented at each lag and wavenumber.

$$C = \text{sech}(aL^b k^c), \quad (2)$$

where  $C$  is the coherence and  $a$ ,  $b$ , and  $c$  are empirically derived constants. Here,  $L$  is the lag time in hours and  $k$  is the wavenumber in inverse meters.

The constants are derived from the data as follows:

- Compute the inverse hyperbolic secant of the coherence at each wavenumber and lag.
- Compute a two-independent variable linear least squares fit of the logarithm of the result from step 1 against the logarithms of lag and wavenumber. The constant will be  $\ln a$ , and the coefficients will be  $b$  and  $c$ , respectively.
- Iteratively adjust  $a$ ,  $b$ , and  $c$  to minimize the maximum or rms difference between the model and the measured data as desired.

The model and the measurements agree well (Table 1), and, in general, the differences are explainable. At  $k = 0$  the model predicts  $C = 1$  identically for all lags, as one would intuitively expect. The actual data are not perfectly coherent at  $k = 0$ , but the data have finite bandwidth and thus the  $k = 0$  bin includes data up to  $k_N/N$  where  $k_N$  is the Nyquist wavenumber and  $N$  is the number of points in the spectrum.

At a lag of 2 h, the model does not handle the smaller

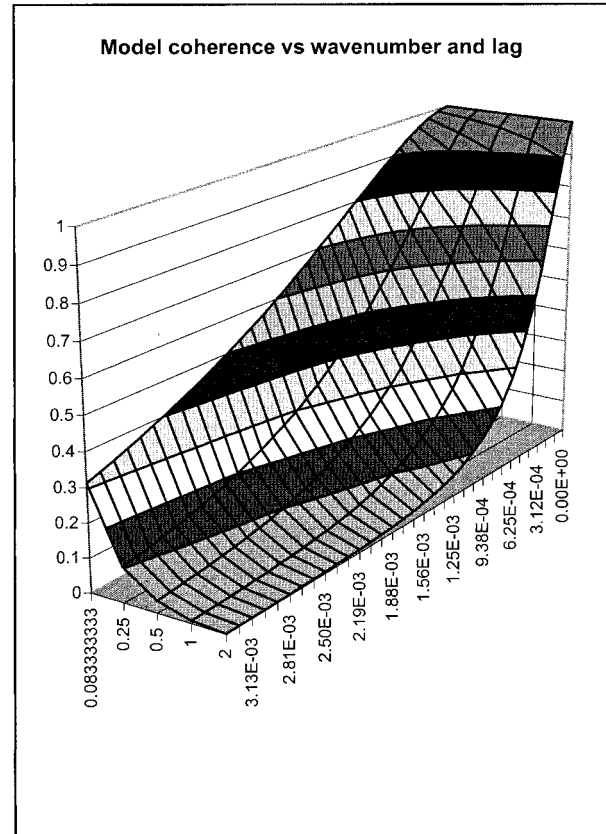


FIG. 6. Coherence of the  $u$  component as a function of vertical wavenumber and time lag from the hyperbolic secant model using the raw data. The equation for the model is  $C = \text{sech}(aL^b k^c)$ . The values of the coefficients are  $a = 498$ ,  $b = 0.440$ , and  $c = 0.791$ .

wavenumbers as well as it does smaller lags and larger wavenumbers. At these longer lag times and larger scales of motion, synoptic, diurnal, and wavelike features may play enough of a role here to reduce the effectiveness of the model. At the smallest lag, 5 min, the larger wavenumbers are not modeled as well. This is due to peculiar characteristics of the profiler noise at this lag, and the model is probably more accurate than the data [see section 4b(3)]. The  $u$ - $v$  asymmetry noted by Merceret (1999) for the 5-min lag does not persist at larger time intervals [see section 4b(1)], and is also probably due to the noise characteristics at small lag and large  $k$ .

#### b. The selected and corrected data

##### 1) THE "NORMAL" SUBSET OF THE DATA

As noted above and in Merceret (1999), the coherence of  $u$  and the coherence of  $v$  at a lag of 5 min (one profile) are not equal when the averaged over the full data set as shown in Fig. 7. This asymmetry does not persist at longer lags as shown in Fig. 8. When the

TABLE 1. Differences between the model and the observations for the  $u$  component of the raw data. The model coefficients are  $a = 498$ ,  $b = 0.440$ , and  $c = 0.791$ . Lag  $N$  denotes a lag time of  $N$  profiles or  $5 N$  min.

$k$ ( $m^{-1}$ )	Lag 1	Lag 3	Lag 6	Lag 12	Lag 24
0.00E+00	0.011	0.028	0.041	0.059	0.112
1.04E-04	0.003	0.012	0.013	0.017	0.033
2.08E-04	0.001	0.004	0.011	0.018	0.024
3.12E-04	-0.002	0.013	0.032	0.058	0.081
4.17E-04	-0.012	-0.002	0.012	0.030	0.043
5.21E-04	-0.024	-0.005	0.008	0.007	0.022
6.25E-04	-0.030	-0.013	-0.010	-0.011	-0.008
7.29E-04	-0.023	0.006	0.017	0.023	0.025
8.33E-04	-0.021	0.020	0.028	0.029	0.024
9.38E-04	-0.017	0.043	0.053	0.051	0.029
1.04E-03	-0.014	0.049	0.057	0.051	0.019
1.15E-03	-0.009	0.058	0.062	0.041	0.007
1.25E-03	-0.012	0.055	0.053	0.044	0.002
1.35E-03	-0.007	0.076	0.070	0.052	0.008
1.46E-03	-0.009	0.083	0.080	0.047	0.004
1.56E-03	-0.002	0.089	0.086	0.045	0.006
1.67E-03	-0.007	0.096	0.085	0.041	0.001
1.77E-03	-0.007	0.102	0.079	0.032	-0.005
1.88E-03	-0.007	0.096	0.075	0.027	-0.003
1.98E-03	-0.014	0.091	0.069	0.032	-0.005
2.08E-03	-0.017	0.084	0.062	0.027	-0.004
2.19E-03	-0.017	0.095	0.063	0.019	-0.006
2.29E-03	-0.029	0.085	0.060	0.015	-0.007
2.40E-03	-0.031	0.080	0.052	0.015	-0.007
2.50E-03	-0.037	0.067	0.041	0.010	-0.008
2.60E-03	-0.045	0.066	0.039	0.009	-0.009
2.71E-03	-0.054	0.064	0.039	0.007	-0.006
2.81E-03	-0.052	0.064	0.036	0.003	-0.008
2.92E-03	-0.062	0.061	0.032	0.002	-0.008
3.02E-03	-0.068	0.061	0.031	0.003	-0.008
3.13E-03	-0.075	0.052	0.026	-0.001	-0.009
3.23E-03	-0.092	0.045	0.022	-0.003	-0.010
3.33E-03	-0.102	0.038	0.020	-0.004	-0.011

“normal” subset is averaged, the asymmetry is minimal even at the smallest lag as shown in Fig. 9.

The hyperbolic secant model works well for both datasets, full and normal, but the coefficients of the best fit differ as shown in Table 2. In addition, the coefficients for  $u$  differ significantly from those for  $v$ , even when Lag 1 is excluded. After correcting the data for instrument noise as described in the next section, model coefficients may be obtained that fit both components well, and it is even possible to fit both datasets with the same set of coefficients as shown in Table 3.

2) APPLYING THE CORRECTION

The correction has two adjustable parameters,  $\beta$  and  $k_0$ . An obvious starting point for applying the correction is to use the observed slope of the power spectrum in log-log coordinates for  $\beta$ . The wavenumber at which the power spectrum begins to flatten out, or that at which the coherence decays to 0.5 for a lag of one profile can be used as the first estimate of  $k_0$ .

The slope of the power spectrum is somewhat dependent on how much of the spectrum is used. If the whole spectrum is used, including the largest and smallest wavenumbers where the spectrum deviates from a pure power law, the result is  $\beta = 2.09$  for the full dataset and 2.15 for the normal set. If the center of the spectrum is isolated, the result is  $\beta = 2.50$  for the full dataset and 2.53 for the normal set. From Merceret (1999), the initial values for  $k_0$  are  $0.00234 m^{-1}$  for  $u$  and  $0.00177 m^{-1}$  for  $v$  over the entire dataset. For the normal set, the values are both equal to about  $0.002 m^{-1}$ .

Using these values as starting points,  $\beta$  and  $k_0$  were adjusted to improve the goodness of fit for the coherence model. After finding the optimum values for the model coefficients,  $a$ ,  $b$ , and  $c$ , the correction parameters were adjusted in small increments to reduce the maximum or rms difference between the model and the corrected

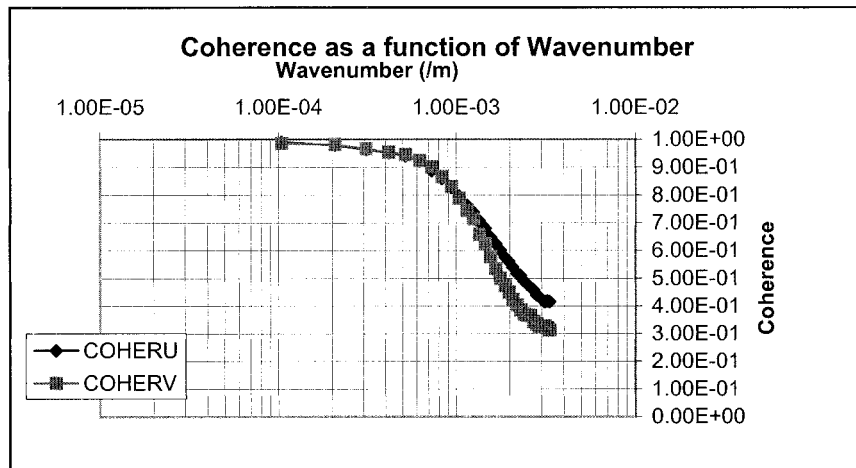


FIG. 7. Coherence for 5-min lag for the complete dataset. The set comprises 93 days containing 23 045 profiles.

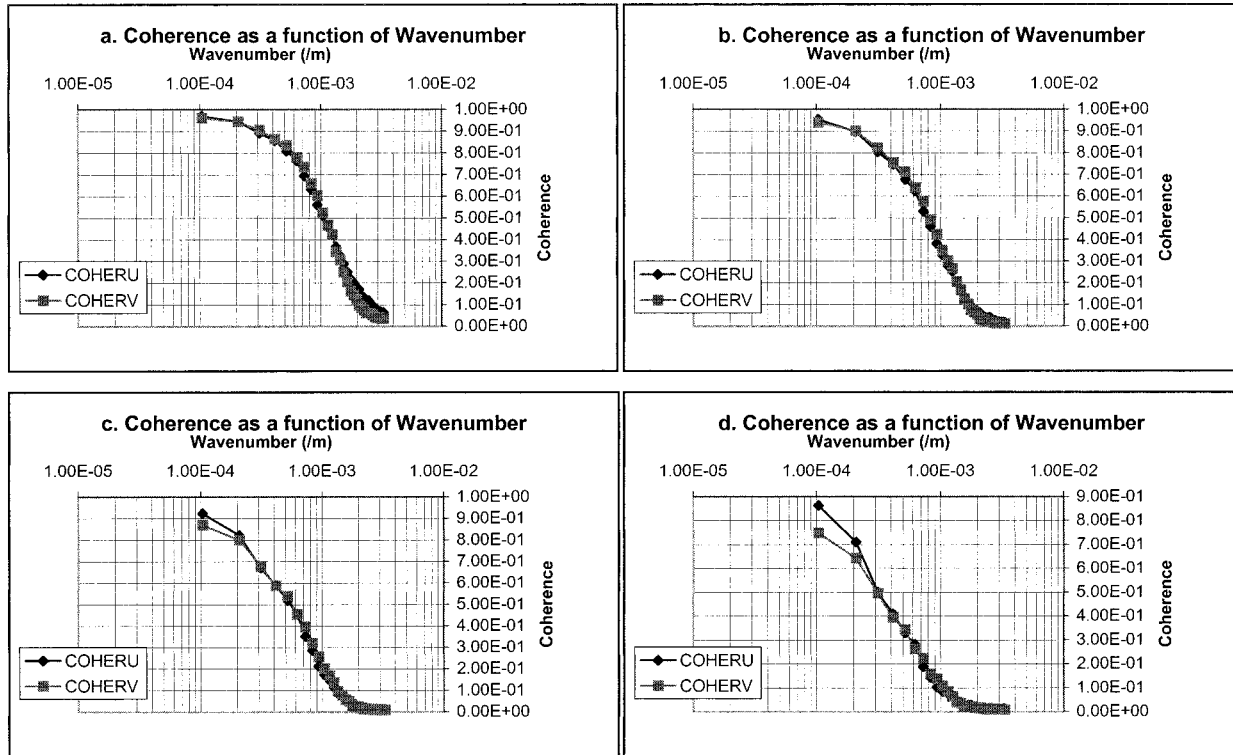


FIG. 8. Same as Fig. 7 for longer lag times. The number of profiles varies but is greater than 20 000 in all cases. (a) is a 15-min lag, (b) is 30 min, (c) is 1 h, and (d) is 2 h.

data. The model coefficients were then reoptimized. This process was repeated until no further improvement could be obtained. The process appeared to be relatively insensitive to changes in  $\beta$  over the range from 2.2 to 2.6, but changes in  $k_0$  were always significant.

### 3) RESULTS FOR THE CORRECTED DATA

The model fits the corrected data well as shown in Table 4 for the full dataset. The optimum correction parameters are  $\beta = 2.4$  for both the full and normal datasets. The values of  $k_0$  for  $u$  and  $v$ , respectively, are 0.0027 and 0.0021  $\text{m}^{-1}$  for both datasets. The model coefficients for the corrected data are significantly different from those for the raw data. The correction process allows the  $u$  and  $v$  components to be modeled isotropically, which is to be expected if we are actually modeling the atmosphere rather than an idiosyncrasy of the profiler. The model and the corrected measured coherences differ by less than 0.1 throughout the entire wavenumber and lag domain excluding lag 1 (5 min).

Lag 1 was omitted in the process used to generate these results since the correction applied to lag 1 (5 min) generated coherences greater than unity at large wavenumbers. This means that one of the assumptions of the correction scheme is not valid, at least at that lag. A detailed reexamination of the lag-1 coherence spectra suggested that the system noise in the DRWP has some

coherence over a 5-min period (adjacent profiles) at the larger wavenumbers. This is due to two features of the data processing algorithm as described by Schumann et al. (1999). First, the algorithm uses a three-point temporal median filter that would correlate noise for one or two lags (5–10 min), but not longer. At larger lags, this effect would not appear. Second, the algorithm “propagates” the previous wind value (designated the “first guess”) when the signal-to-noise ratio is too poor to permit a new wind to be derived. Although the quality control process discarded winds for which the first guess was propagated for more than 30 min, propagation for shorter periods was allowed. An inspection of the data confirmed that most first-guess propagations were for 10 min or less, and that they occurred in adjacent gates or, equivalently, the higher wavenumbers. Based on the foregoing analysis, it appears likely that the model values for the corrected coherences are probably more accurate at lag 1 than either the raw or corrected coherence at that lag.

### c. The relation between lifetime and vertical scale

The relationship between the coherence scale and the coherence time can be derived easily from the model. The coherence scale is the scale of motion at which the coherence falls to a predetermined value  $\varepsilon$ . In Merceret (1999) the value used was 0.5. The value of 0.25 is

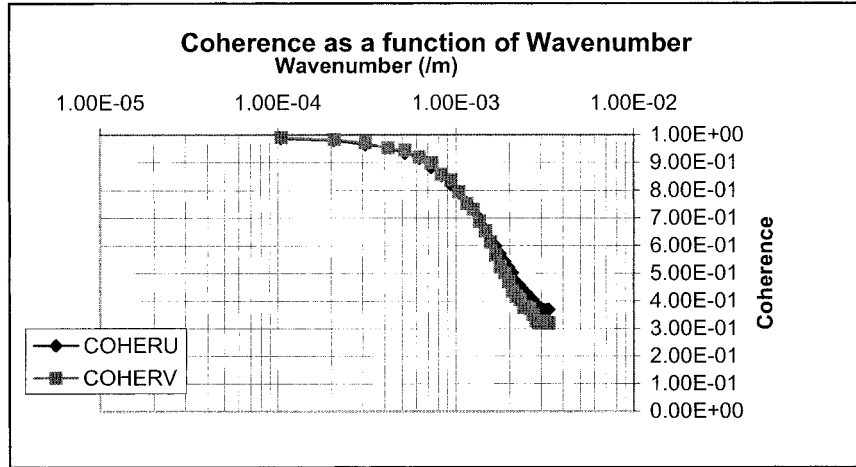


FIG. 9. Same as Fig. 7 for the normal data at a 5-min lag. The sample contains 10 727 profiles from 44 days.

consistent with much of the literature in which “coherence” is the square root of the quantity denoted by that name here. Given the model  $C = \text{sech}(aL^b k^c)$ , then the coherence scale  $\lambda = 1/k_c$ , where the coherence wavenumber  $k_c$  may be determined for any given coherence time  $\tau$  from

$$\varepsilon = \text{sech}(a\tau^b k_c^c), \tag{3}$$

resulting in  $k_c = [\text{sech}^{-1}(\varepsilon)/(a\tau^b)]^{1/c}$  or

$$\lambda = [(a\tau^b)/\text{sech}^{-1}(\varepsilon)]^{1/c}. \tag{4}$$

This may be inverted to

$$\tau = [\text{sech}^{-1}(\varepsilon)\lambda^c/a]^{1/b}. \tag{5}$$

The model parameters were computed for both the normal subset and the total data sample. The computations were optimized several different ways.

- The raw data were processed with and without lag 1 (5 min).
- The corrected  $u$  and  $v$  component coefficients were optimized separately.
- The corrected  $u$  and  $v$  coefficients were set equal and jointly optimized.
- The normal and total dataset coefficients were set equal and jointly optimized.

TABLE 2. Hyperbolic secant model coefficients for the raw data.

Set	Lag 1	Component	$a$	$b$	$c$
Total	Included	$u$	498.000	0.440	0.791
Total	Included	$v$	613.000	0.440	0.798
Normal	Included	$u$	604.000	0.435	0.818
Normal	Included	$v$	639.000	0.368	0.830
Total	Excluded	$u$	539.000	0.427	0.792
Total	Excluded	$v$	612.000	0.482	0.798
Normal	Excluded	$u$	605.000	0.414	0.817
Normal	Excluded	$v$	680.000	0.410	0.829

- The coefficients for  $u$  and  $v$  in both corrected datasets were set equal and jointly optimized.

The resulting coefficients were used to generate curves of  $\tau$  versus  $\lambda$  for each case. The results fell into two families, one for the raw data and one for the corrected data. Despite substantial differences in the values of the coefficients for these two families, the  $\tau$  versus  $\lambda$  curves differed little. The minimum, maximum, and mean lifetime obtained from the various optimizations at each vertical scale is presented in Fig. 10 for  $\varepsilon = 0.5$ . The minimum and maximum values differ by less than a factor of 2 although  $a$  ranged from 246 to 680,  $b$  from 368 to 482, and  $c$  from 0.694 to 0.830. That is because  $a$  and  $c$  were positively correlated ( $r^2 = 0.96$ ) and have opposite effect on the value of  $\tau$ . Figure 11 presents the corresponding results for  $\varepsilon = 0.25$ . The latter lifetimes are about a factor of 3 longer.

*d. Interpretation*

The model provides a quantitative estimate of the coherence as a function of wavenumber and time lag that matches the data remarkably well given its purely

TABLE 3. Hyperbolic secant model coefficients for the corrected data excluding lag 1. The “Nor = Tot” column indicates whether the fit was constrained to generate equal coefficients for the total and normal datasets.

Set	Nor = Tot	Component	$a$	$b$	$c$
Total	No	$u$	282.000	0.450	0.706
Total	No	$v$	282.000	0.450	0.706
Normal	No	$u$	330.000	0.413	0.743
Normal	No	$v$	330.000	0.413	0.743
Total	Yes	$u$	305.000	0.385	0.730
Total	Yes	$v$	305.000	0.385	0.730
Normal	Yes	$u$	305.000	0.385	0.730
Normal	Yes	$v$	305.000	0.385	0.730

TABLE 4. Differences between the model and the observations for the  $u$  component of the corrected data. The model coefficients are  $a = 282$ ,  $b = 0.450$ , and  $c = 0.706$ . Lag  $N$  denotes a lag time of  $N$  profiles or  $5N$  minutes.

$k$ ( $m^{-1}$ )	Lag 1	Lag 3	Lag 6	Lag 12	Lag 24
0.00E+00	0.011	0.028	0.041	0.059	0.112
1.04E-04	0.000	0.003	-0.003	-0.012	-0.017
2.08E-04	-0.007	-0.014	-0.019	-0.030	-0.048
3.12E-04	-0.014	-0.011	-0.006	0.003	0.009
4.17E-04	-0.029	-0.031	-0.029	-0.024	-0.019
5.21E-04	-0.047	-0.038	-0.035	-0.043	-0.028
6.25E-04	-0.060	-0.049	-0.053	-0.056	-0.048
7.29E-04	-0.060	-0.033	-0.023	-0.015	-0.005
8.33E-04	-0.066	-0.022	-0.011	-0.004	0.000
9.38E-04	-0.072	0.001	0.018	0.025	0.012
1.04E-03	-0.079	0.005	0.025	0.029	0.005
1.15E-03	-0.086	0.012	0.031	0.022	-0.004
1.25E-03	-0.101	0.007	0.023	0.029	-0.008
1.35E-03	-0.109	0.028	0.044	0.041	0.001
1.46E-03	-0.126	0.034	0.058	0.037	-0.003
1.56E-03	-0.133	0.040	0.067	0.038	0.001
1.67E-03	-0.155	0.048	0.070	0.036	-0.004
1.77E-03	-0.172	0.055	0.065	0.027	-0.011
1.88E-03	-0.193	0.047	0.062	0.022	-0.008
1.98E-03	-0.221	0.040	0.057	0.030	-0.011
2.08E-03	-0.245	0.030	0.050	0.025	-0.010
2.19E-03	-0.268	0.048	0.055	0.015	-0.012
2.29E-03	-0.310	0.033	0.054	0.011	-0.015
2.40E-03	-0.340	0.026	0.043	0.012	-0.014
2.50E-03	-0.374	0.004	0.028	0.006	-0.017
2.60E-03	-0.416	0.003	0.026	0.003	-0.020
2.71E-03	-0.464	0.001	0.030	0.002	-0.015
2.81E-03	-0.491	0.003	0.028	-0.006	-0.019
2.92E-03	-0.546	0.000	0.023	-0.008	-0.020
3.02E-03	-0.593	0.002	0.024	-0.005	-0.021
3.13E-03	-0.652	-0.017	0.016	-0.014	-0.025
3.23E-03	-0.735	-0.031	0.009	-0.019	-0.029
3.33E-03	-0.805	-0.049	0.006	-0.023	-0.034

empirical nature. The author has been unable to find any physical basis for the model, but it has the asymptotic properties one would expect at both large and small wavenumber and lag for turbulent flows. It provides a convenient practical tool for estimating lifetimes as a function of scale for any chosen coherence, or coherence as a function of lag and wavenumber provided its limitations are kept in mind. The data were limited to the winter season over central Florida and did not include cases in which significant coherent gravity wave activity was detected.

### 5. Summary and conclusions

Measurements of the coherence between KSC DRWP wind profiles separated in time by from 5 min to 2 h were presented. The profiles spanned the altitude range from 6811 to 16 261 m. There were 93 days and more than 20 000 profiles in the dataset.

A method of correcting the measured coherence for the incoherent instrument noise was derived and applied to the data. The correction procedure produced spurious results for the 5-min lag time at the larger wavenumbers. This appears to result from instrument noise, which is coherent over the 5-min lag due to the signal processing used in the KSC profiler. At lags equal to or greater than 15 min, the correction worked well.

An empirical model of the coherence function for wavenumbers from 0 to  $0.0033 m^{-1}$  at lag times from 0.083 to 2 h was developed and was applied to both the raw data and the corrected data. This hyperbolic secant model, presented in Eq. (2), fit the data well in both cases. The differences between the data and the model were less than 0.1 at all wavenumbers and lags except for lag 1 (5 min) at the higher wavenumbers and lag 24

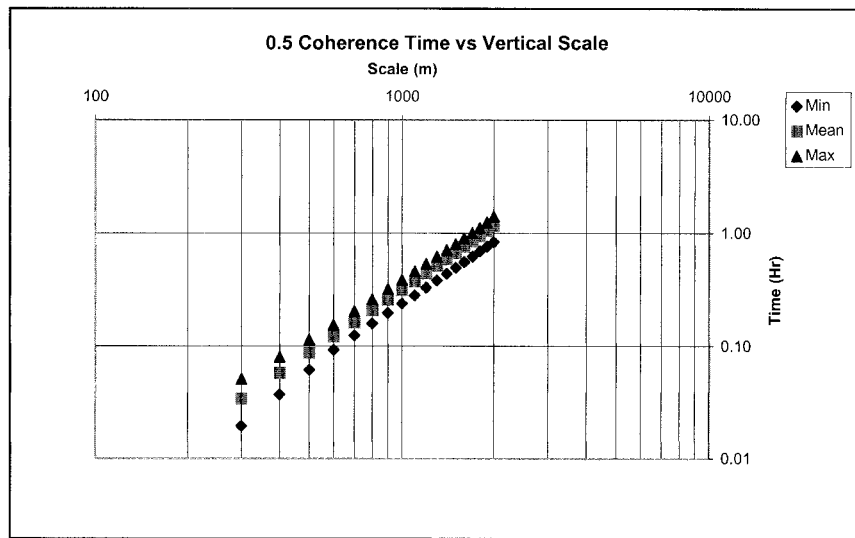


FIG. 10. Coherence time ( $\tau$ ) vs vertical scale ( $\lambda$ ) for a coherence threshold ( $\epsilon$ ) of 0.5. The least squares fit for the mean is  $\tau = 8 \times 10^{-7} \lambda^{1.863}$ , where  $\tau$  is measured in hours and  $\lambda$  in meters.

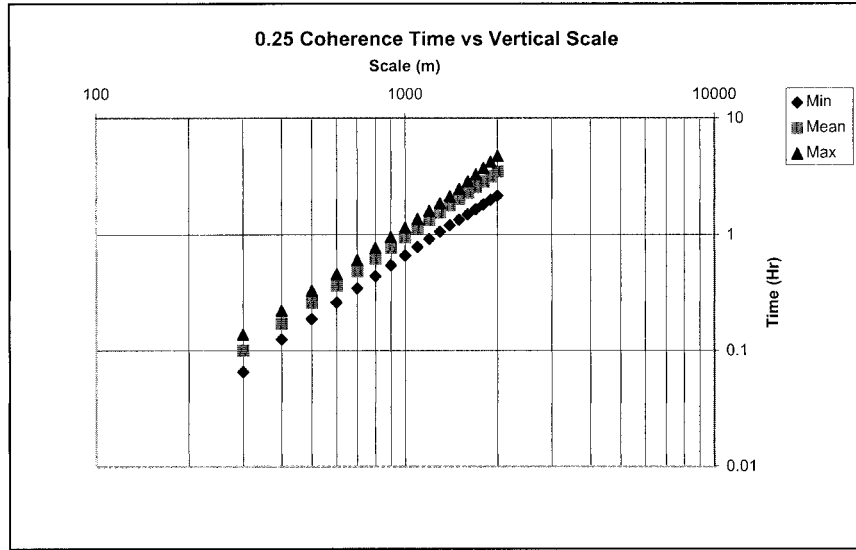


FIG. 11. Coherence time ( $\tau$ ) vs vertical scale ( $\lambda$ ) for a coherence threshold ( $\epsilon$ ) of 0.25. The least squares fit for the mean is  $\tau = 2 \times 10^{-6} \lambda^{1.871}$ , where  $\tau$  is measured in hours and  $\lambda$  in meters.

(2 h) at the lowest wavenumber. The lag-1 data are contaminated by coherent noise. The lag-24 large-scale data may include synoptic, diurnal, or wave components.

Using the model, a relationship between the lifetime of a feature and its vertical scale was derived and presented in Eq. (5). The quantitative results for the raw and the corrected data did not differ significantly. Changing the coherence threshold for the definition of “lifetime” from 0.5 to 0.25 increased the lifetime by a factor of about 3.

This work was undertaken to quantify the lifetime of midtropospheric features as a function of their vertical scale. The information was sought to determine the resolution required of upper-air wind instruments supporting spaceflight operations. The model provides the necessary information for the winter season in the absence of significant coherent gravity wave activity. It should also be of interest to those designing upper-air measurement or modeling programs where temporal and vertical resolution are design parameters or constraints. The technique for correcting coherence measurements is generally applicable to any phenomenon that exhibits a power law spectrum, a common feature in many branches of geophysics.

*Acknowledgments.* The author thanks Dr. Gregory Taylor for suggesting that first-guess propagation could contribute to the correlation of the noise at lag 1. Suggestions by anonymous reviewers led to significant improvement in the paper. They are acknowledged with gratitude.

APPENDIX

Derivation of the Correction of Coherence Spectra for Instrument Noise

The following derivation is done in the time and frequency domains because that notation looks more familiar. The result is applied in the  $z$  and  $k$  domains.

Let  $s(t)$  be the signal with Fourier transform  $S(f)$  and known coherence spectrum. Let  $n(t)$  be the noise with Fourier transform  $N(f)$ . For this derivation, the noise will be assumed to be incoherent both with itself and with the signal. Given two functions  $x(t)$  and  $y(t)$  with Fourier transforms  $X(f)$  and  $Y(f)$ , respectively, the coherence spectrum between them is given by

$$C_{xy}(f) = \frac{\langle [X(f)Y^*(f)][Y(f)X^*(f)] \rangle}{\langle [X(f)X^*(f)][Y(f)Y^*(f)] \rangle}, \quad (A1)$$

where  $\langle x \rangle$  denotes the ensemble average of  $x$  and the asterisk denotes the complex conjugate. Now let  $x(t) = s(t) + n(t)$  and let  $y(t, \tau)$  be the time-lagged value  $s(t - \tau) + n(t - \tau)$ . Since the Fourier transform is a linear operator,  $X(f) = S(f) + N(f)$  and  $Y(f) = S'(f) + N'(f)$  where the apostrophe denotes the transform of the lagged function.

For convenience, drop the explicit arguments. The essential products are as follows:

$$XX^* = SS^* + SN^* + NS^* + NN^*. \quad (A2)$$

When this is averaged, the middle two terms vanish because the noise and the signal are mutually incoherent. Thus  $\langle XX^* \rangle = \langle SS^* \rangle + \langle NN^* \rangle$  and similarly,

$$\langle YY^* \rangle = \langle S'S'^* \rangle + \langle N'N'^* \rangle. \quad (A3)$$

The cross product is given by

$$XY^* = SS'^* + SN'^* + NS'^* + NN'^*. \quad (\text{A4})$$

When this is averaged, the middle two terms again vanish because the noise and the signal are mutually incoherent. The last term vanishes because the noise, by hypothesis, has zero autocorrelation. Thus,

$$\langle XY^* \rangle = \langle SS'^* \rangle \text{ and } \langle YX^* \rangle = \langle S'S'^* \rangle, \quad (\text{A5})$$

then

$$C_{xy} = \langle SS'^* \rangle \langle S'S'^* \rangle / (\langle SS'^* \rangle + \langle NN'^* \rangle) (\langle S'S'^* \rangle + \langle N'N'^* \rangle). \quad (\text{A6})$$

If the signal and noise signals are stationary, then  $\langle S'S'^* \rangle = \langle SS'^* \rangle$ ,  $\langle N'N'^* \rangle = \langle NN'^* \rangle$  and  $\langle SS'^* \rangle = \langle S'S'^* \rangle$ . Under these circumstances,

$$C_{xy} = \langle SS'^* \rangle^2 / (\langle SS'^* \rangle^2 + \langle NN'^* \rangle^2 + 2\langle SS'^* \rangle \langle NN'^* \rangle) \quad (\text{A7})$$

If we normalize by dividing the numerator and denominator by  $\langle SS'^* \rangle^2$ , we get

$$C_{xy} = (\langle SS'^* \rangle^2 / \langle SS'^* \rangle^2) / (1 + \langle NN'^* \rangle / \langle SS'^* \rangle)^2, \quad (\text{A8})$$

where the numerator is now the coherence of the signal in the absence of noise.

Consequences:

(a) For perfectly coherent data, the measured coherence falls to 0.5 when the noise to signal ratio  $\langle NN'^* \rangle / \langle SS'^* \rangle$  reaches  $\sqrt{2} - 1$  or, more conventionally, the signal-to-noise ratio falls to  $1/(\sqrt{2} - 1)$ . This is a signal-to-noise ratio of 2.414 or 3.83 dB.

(b) For perfectly coherent data, the signal-to-noise ratio falls to unity (0 dB) when the coherence falls to 0.25.

(c) Coherences less than unity scale the same as unity coherences. The effect of noise does not depend on the degree to which the signal is coherent.

(d) If we assume that the noise spectrum is independent of frequency ("white noise") and that the signal spectrum obeys a power law  $\langle SS'^* \rangle \propto (f/f_0)^{-\beta}$  ("red noise") typical of atmospheric signals, then we can write the coherence equation (omitting the  $xy$  subscripts for simplicity) as

$$C_{\text{measured}}(f) = C_{\text{actual}}(f) / [1 + (\sqrt{2} - 1)(f/f_0)^\beta]^2, \quad (\text{A9})$$

where  $f_0$  is the frequency at which the measured coherence falls to 0.5 for a perfectly coherent signal. Obviously, this may be inverted to recover the actual coherence spectrum from a measured spectrum if  $f_0$  is known. For our application,  $t$  is replaced by the vertical coordinate  $z$ , and  $f$  is replaced by the vertical wavenumber  $k$ . In that case,

$$C_{\text{actual}}(k) = C_{\text{measured}}(k) [1 + (\sqrt{2} - 1)(k/k_0)^\beta]^2. \quad (\text{A10})$$

## REFERENCES

- Alexander, P., and A. De La Torre, 1999: The interpretation of saturated spectra as observed from atmospheric balloon measurements. *J. Appl. Meteor.*, **38**, 334–342.
- Allen, S. J., and R. A. Vincent, 1995: Gravity wave activity in the lower atmosphere: Seasonal and latitudinal variations. *J. Geophys. Res.*, **100**, 1327–1350.
- Lumley, J. L., and H. A. Panofsky, 1964: *The Structure of Atmospheric Turbulence*. John Wiley and Sons, 239 pp.
- Merceret, F. J., 1997: Rapid temporal changes of midtropospheric winds. *J. Appl. Meteor.*, **36**, 1567–1575.
- , 1999: The vertical resolution of the Kennedy Space Center 50 MHz wind profiler. *J. Atmos. Oceanic Technol.*, **16**, 1273–1278.
- Nastrom, G. D., T. E. Van Zandt, and J. M. Warnock, 1997: Vertical wavenumber spectra of wind and temperature from high-resolution balloon soundings over Illinois. *J. Geophys. Res.*, **102**, 6685–6701.
- Parzen, E., 1961: Mathematical considerations in the estimation of spectra. *Technometrics*, **3**, 167–190.
- Schumann, R. S., G. E. Taylor, F. J. Merceret, and T. L. Wilfong, 1999: Performance characteristics of the Kennedy Space Center 50-MHz Doppler radar wind profiler using the median filter first-guess data reduction algorithm. *J. Atmos. Oceanic Technol.*, **16**, 532–549.
- Stull, R. B., 1989: *An Introduction to Boundary Layer Meteorology*. Kluwer Academic Publishers, 666 pp.
- Weinstock, J., 1978: On the theory of turbulence in the buoyancy subrange of stably stratified flows. *J. Atmos. Sci.*, **35**, 634–649.
- Wilfong, T. L., S. A. Smith, and R. L. Creasy, 1993: High temporal resolution velocity estimates from a wind profiler. *J. Spacecr. Rockets*, **30**, 348–354.
- , —, and C. L. Crosiar, 1997: Characteristics of high-resolution wind profiles derived from radar-tracked jimspheres and the rose processing program. *J. Atmos. Oceanic Technol.*, **14**, 318–325.